

# RSC Advances

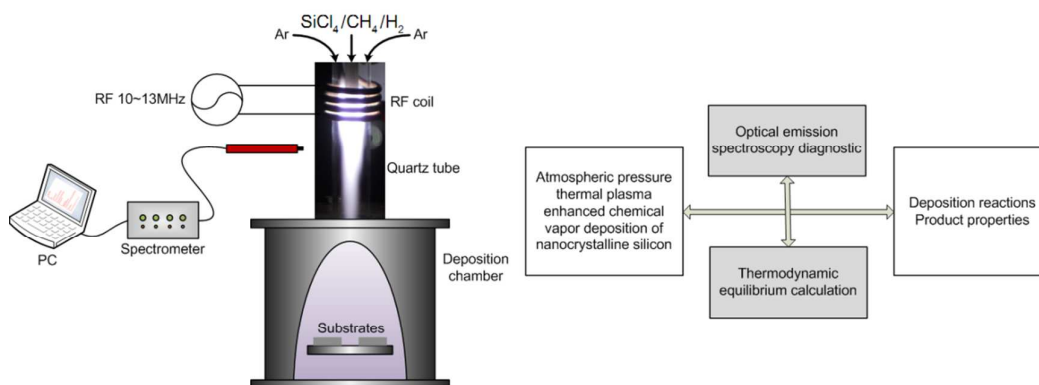


This is an *Accepted Manuscript*, which has been through the Royal Society of Chemistry peer review process and has been accepted for publication.

*Accepted Manuscripts* are published online shortly after acceptance, before technical editing, formatting and proof reading. Using this free service, authors can make their results available to the community, in citable form, before we publish the edited article. This *Accepted Manuscript* will be replaced by the edited, formatted and paginated article as soon as this is available.

You can find more information about *Accepted Manuscripts* in the [Information for Authors](#).

Please note that technical editing may introduce minor changes to the text and/or graphics, which may alter content. The journal's standard [Terms & Conditions](#) and the [Ethical guidelines](#) still apply. In no event shall the Royal Society of Chemistry be held responsible for any errors or omissions in this *Accepted Manuscript* or any consequences arising from the use of any information it contains.



Optical emission spectroscopy and thermal equilibrium analysis were implemented to study the plasma enhanced chemical vapor deposition of nanocrystalline silicon.

# Optical emission spectroscopy diagnostic and thermodynamic analysis of thermal plasma enhanced nanocrystalline silicon CVD process

Tengfei Cao, Haibao Zhang, Binhang Yan, Wei Lu and Yi Cheng\*

## Abstract

Nanocrystalline silicon is a promising alternative for the conventional crystalline silicon materials in the photovoltaic industry because of its better photostability and easy fabrication. However, the low deposition rates of conventional nanocrystalline silicon fabrication processes hamper its application in industry. Thermal plasma has been used to successfully realize the high rate deposition of nanocrystalline silicon in this work. Optical emission spectroscopy (OES) diagnostic and thermodynamic equilibrium calculation are carried out to better understand the mechanism of deposition reactions and the effect of  $\text{SiCl}_4$  input rate on nanocrystalline silicon deposition rate and product properties. Emission lines of atomic silicon, atomic hydrogen and atomic argon are observed. The results show that the amount of silicon related species in the gas phase is the main factor affecting the deposition process, which has a linear relationship with nanocrystalline silicon deposition rate, grain size and crystalline fraction at the high  $\text{H}_2$  dilution ratio of the deposition system.

## Introduction

Hydrogenated nanocrystalline silicon (nc-Si:H) is a thin-film semiconductor which has attracted much attention during the last decade for its promising applications in the production of

solar cells, thin film transistors (TFT) and image sensors.<sup>1-4</sup> nc-Si:H has a better photostability and higher absorption capability in the near-infrared wavelength range than hydrogenated amorphous silicon (a-Si:H) because of the existence of crystalline phase in the material.<sup>5,6</sup> However, the low deposition rates of the conventional cold plasma enhanced nc-Si:H deposition processes hampered its application in photovoltaic industry.

Thermal plasma has the feature of high energy and high reactive species density thus offers very high fluxes of matter and energy in nanoscale synthesis.<sup>7</sup> It has been used as an efficient technique for high rate generation of nanoparticles and nanostructures over the last twenty years.<sup>8-12</sup> K. K. Ostrikov et al.<sup>13</sup> has discussed the basic principles of plasma nanoscience and introduced the latest application of plasma in nanoscale materials fabrication. Materials can be evaporated rapidly in thermal plasma and the rapid quenching of the plasma can also promote nucleation. Our previous work has successfully realized the high rate deposition of nc-Si:H thin films using an atmospheric pressure thermal plasma enhanced CVD (APTPECVD) process<sup>14</sup>, where the inductively coupled plasma (ICP) was particularly appropriate for high-purity product deposition for the absence of electrode. SiCl<sub>4</sub> diluted by H<sub>2</sub> was used as precursor. A nc-Si:H deposition rate up to 9.78 nm s<sup>-1</sup> was achieved, which is much higher than the maximum deposition rate as reported<sup>1, 15</sup>. The silicon deposition rate and product properties of SiCl<sub>4</sub>-H<sub>2</sub> system exhibit strong dependence on the input rate of SiCl<sub>4</sub> and the dilution ratio H<sub>2</sub>/SiCl<sub>4</sub>. Optical emission spectroscopy (OES) diagnostic and equilibrium calculation has been carried out in this work to better understand this relationship.

OES is a non-intrusive diagnostic technique, which can monitor the concentration change of reactive species and give multiple valuable information of plasma. The optical emission intensities

of silicon atom and  $H_2$  as a function of  $SiH_4$  percentage in  $SiH_4$ -Ar mixture glow discharge have been measured by Kampas.<sup>16</sup> The mechanisms of excited species formation in the  $SiH_4$ - $H_2$ ,  $SiF_4$  and  $SiF_4$ - $H_2$  plasma systems have been elucidated by Cicala et al.<sup>17</sup> Silicon hydrogenation by RF inductive thermal plasma has been studied via OES by Bourg et al.<sup>18</sup> and the electron density and electron temperature in the plasma was calculated. The temporal behavior of a pure  $SiH_4$  plasma has been characterized by Feitknecht et al.<sup>19</sup> and the kinetics of the emission lines of  $SiH^*$  and  $H_\alpha$  was reported. Yokoyama et al.<sup>20</sup> and Fukuda et al.<sup>21</sup> have correlated OES intensity with deposition rate and product properties in  $SiH_4$ - $H_2$ - $NH_3$  and  $SiH_4$ - $H_2$  PECVD respectively. Nevertheless, less work has been done on silicon deposition from  $SiCl_4$ - $H_2$  mixture under atmospheric thermal plasma. In this study, OES is applied to explore the deposition reactions in the  $SiCl_4$ - $H_2$ -Ar APTPECVD process and the mechanisms of excited species formation.

Thermodynamically calculated states have been used to aid in explaining experimental data from chlorosilane related processes in the literature. The equilibrium Si-H-Cl system depends only upon the initial and final states of the system.<sup>22</sup> Sirtl et al.<sup>23</sup> presented a general discussion to understand the complexity of reaction mechanisms existing for silicon deposition from  $SiCl_4$ - $H_2$  and  $SiHCl_3$ - $H_2$  mixtures. Eichfeld et al.<sup>24</sup> used the gas phase equilibrium model of the  $SiCl_4$ - $H_2$  system to analyze the gas phase limitations on the growth of silicon nanowires under atmospheric pressure CVD conditions. However, the temperature ranges considered in those papers are much lower than the temperature of thermal plasma. In this work, the effects of  $SiCl_4$  input rate on the deposition rate and properties of nc-Si:H were investigated via the equilibrium calculation of Si-H-Cl at the high temperature conditions of RF thermal plasma while the thermodynamic equilibrium assumption of the gas phase in the plasma zone can be reasonably made in the high

temperature field, especially when the gas stays in the ICP thermal plasma with a long enough residence time. The species residence time in the thermal plasma zone was estimated to be 6.5 ms in this work. Bourg et al.<sup>18</sup> has validated the equilibrium assumption of the ICP thermal plasma deposition system with OES diagnostic. And Yan et al.<sup>25</sup> has validated the equilibrium assumption of a lower temperature milliseconds process by comparison of gas phase compositions measured by experiments and calculated under equilibrium assumption. In this work, the equilibrium assumption of the plasma zone is validated by the correlation of OES analysis with equilibrium calculation results.

## Results and discussion

### 1. Effect of SiCl<sub>4</sub> input rate on gas phase composition detected by OES diagnostic

The optical emission spectrum of the OES diagnostic experimental system at the SiCl<sub>4</sub> input rate of 0.26 mol h<sup>-1</sup> is shown in Fig. 1. Emission lines of reactive species including atomic silicon, atomic hydrogen and atomic argon are observed. Emission bands of excited fragments such as SiCl<sub>x</sub> ( $x = 1, 2$  or  $3$ ) observed in other SiCl<sub>4</sub> plasma decomposition processes<sup>26-28</sup> are not identified in this system. The amount of those fragments may be very small because of the sufficient ability of the ICP RF plasma to decompose precursors to produce atomic radicals. On the other hand, the emission bands of those excited fragments have a relatively low signal to noise ratio, which would make them difficult to be identified compared with the emission lines of atomic silicon.

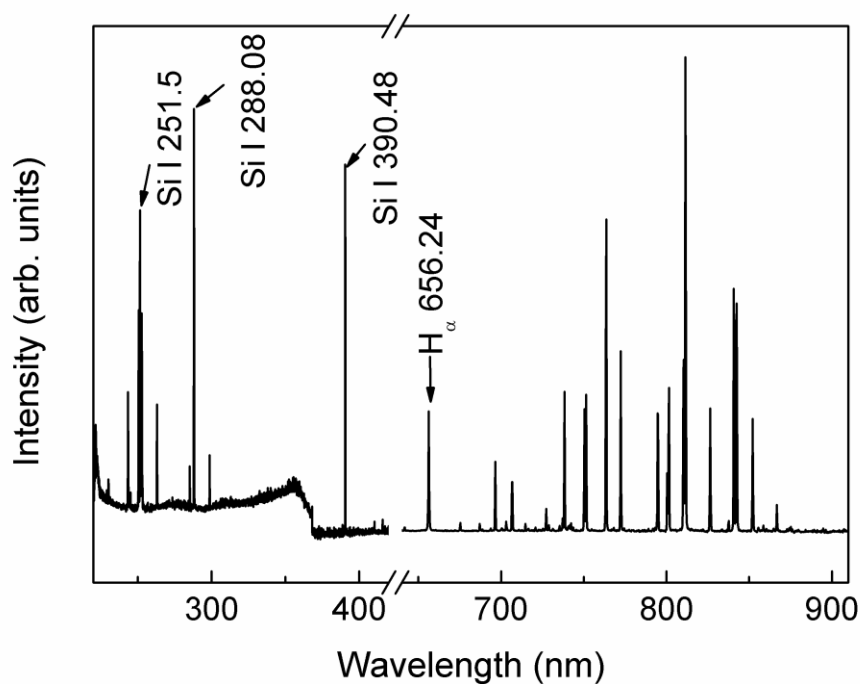


Fig. 1 The optical emission spectrum of the OES diagnostic experimental system at the  $\text{SiCl}_4$  input rate of  $0.26 \text{ mol h}^{-1}$ : the main emission lines of atomic silicon and atomic hydrogen are noted on the spectrum.

The effect of  $\text{SiCl}_4$  input rate on the signal intensities of Si (288.08 nm) and  $\text{H}_\alpha$  (656.24 nm) is given in Fig. 2. The Si (288.08 nm) signal intensity does not increase linearly with the  $\text{SiCl}_4$  input rate. It drops a little when the  $\text{SiCl}_4$  input rate is high. The  $\text{H}_\alpha$  signal intensity decreases slightly with increasing  $\text{SiCl}_4$  input rate. Based on the one-electron pathway mechanism of  $\text{SiH}_4$  and  $\text{SiF}_4$ <sup>17</sup>, the formation mechanism of excited species,  $\text{H}^*$  and  $\text{Si}^*$ , in the  $\text{SiCl}_4\text{-H}_2$  plasma system can be deduced as below:





Thus, according to Equation (6), the intensity of the atomic silicon emission is given by

$$I_{\text{Si}} = C_{\text{Si}} k_{\text{Si}} n_{\text{e}} [\text{Si}], \quad (7)$$

where  $C_{\text{Si}}$  is a constant independent of the deposition parameters,  $k_{\text{Si}}$  is the rate constant for excitation of silicon atomic to the excited state,  $n_{\text{e}}$  is the electron concentration in the plasma and  $[\text{Si}]$  is the atomic silicon concentration. According to Equation (1), the intensity of atomic hydrogen emission is given by

$$I_{\text{H}} = C_{\text{H}} k_{\text{H}} n_{\text{e}} [\text{H}_2], \quad (8)$$

where  $C_{\text{H}}$  and  $k_{\text{H}}$  are the constants for hydrogen atom and  $[\text{H}_2]$  is the  $\text{H}_2$  concentration. The intensity ratio  $I_{\text{Si}}/I_{\text{H}}$  is given by

$$I_{\text{Si}}/I_{\text{H}} = \frac{C_{\text{Si}} k_{\text{Si}}}{C_{\text{H}} k_{\text{H}}} \frac{[\text{Si}]}{[\text{H}_2]} \propto [\text{Si}]/[\text{H}_2]. \quad (9)$$

So, the intensity ratio  $I_{\text{Si}}/I_{\text{H}}$  is proportional to the gas phase concentration ratio  $[\text{Si}]/[\text{H}_2]$ .

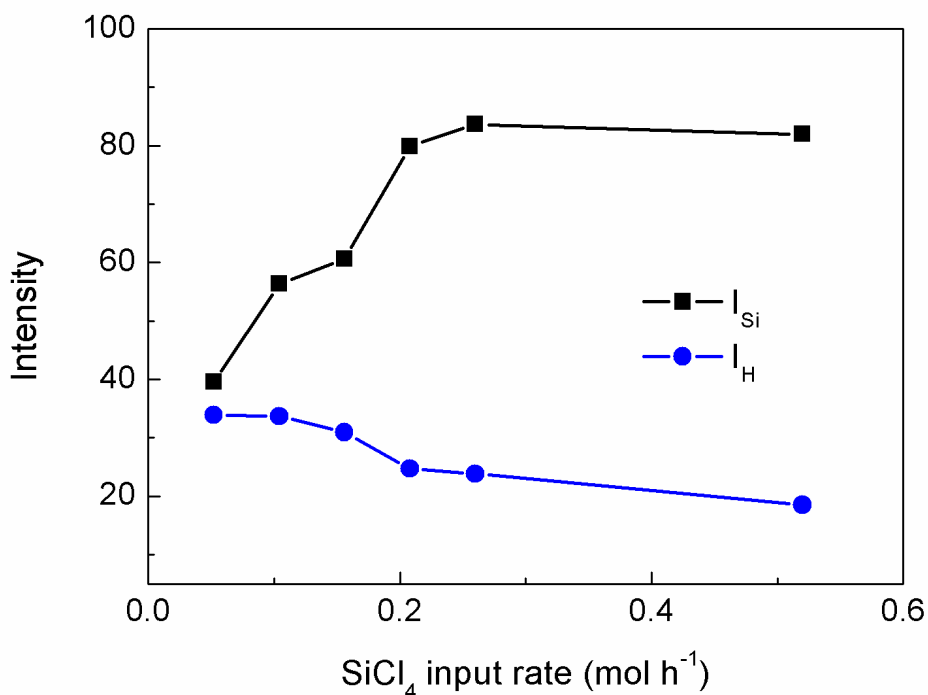


Fig. 2 Effect of SiCl<sub>4</sub> input rate on the signal intensities of Si(288.08 nm) and H<sub>α</sub>(656.24 nm)

The gas phase composition information containing [Si] and [H<sub>2</sub>] is needed in order to understand the influence of SiCl<sub>4</sub> input rate on OES intensity, which can be predicted by thermodynamic equilibrium calculation under equilibrium assumption. The effect of SiCl<sub>4</sub> input rate on the amount of major species in the gas phase is given in Fig. 3 by equilibrium calculation. Atomic silicon is the dominating silicon related species at very low SiCl<sub>4</sub> input rate while SiCl becomes dominating when the SiCl<sub>4</sub> input rate increases. The amount of atomic hydrogen is sufficient to enhance the dissociation of SiCl<sub>4</sub> to form atomic silicon through Equation (3) at very low SiCl<sub>4</sub> input rate, very high H<sub>2</sub> dilution ratio. The amount of atomic hydrogen decreases with increasing SiCl<sub>4</sub> input rate and the dissociation of SiCl<sub>4</sub> stops at SiCl for insufficient atomic hydrogen. The change of [Si] in the gas phase leads to the change of the emission intensity of atomic silicon according to Equation (7). Both atomic hydrogen and H<sub>2</sub> reduce with SiCl<sub>4</sub> input

rate. More atomic hydrogen and  $H_2$  are consumed through Equations (3), (4) and (5) with more  $SiCl_4$  input. And the decrease of  $[H_2]$  results in the decrease of the emission intensity of atomic hydrogen according to Equation (8). HCl is the major chlorine related species and its amount enhances dramatically as more chlorine atoms enter the system.

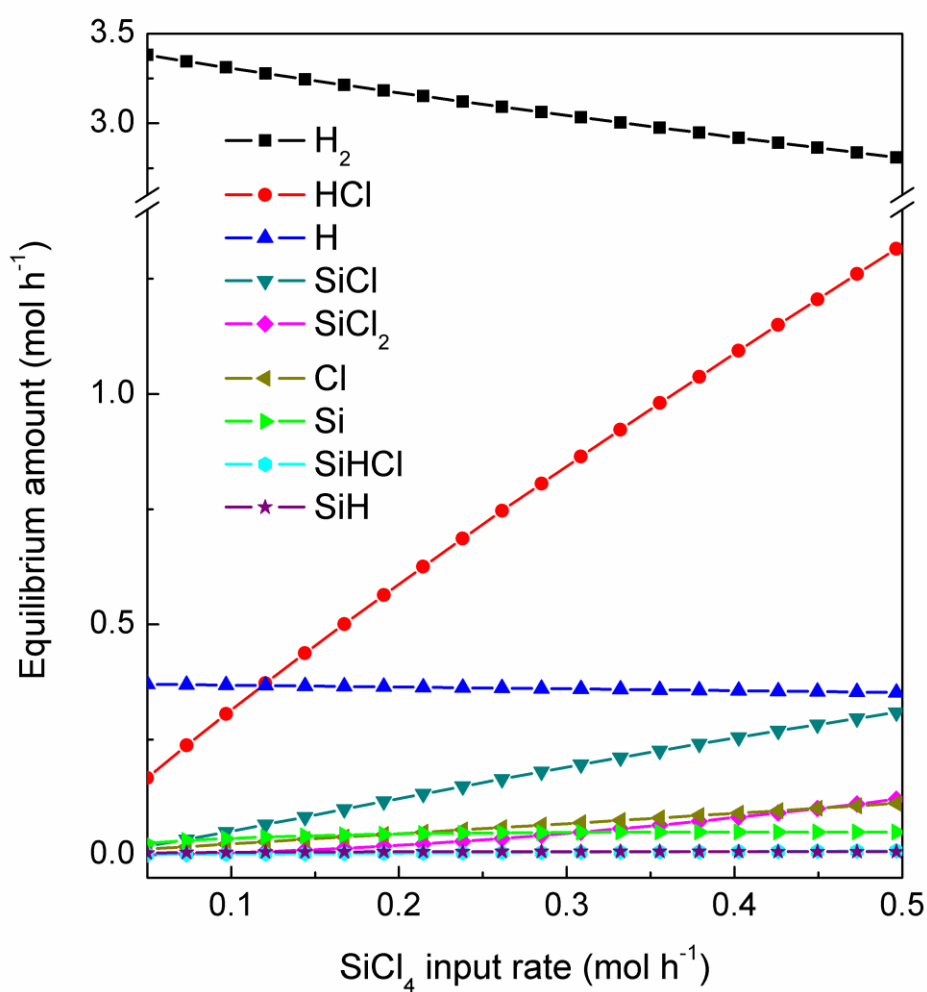


Fig. 3 Gas phase composition at different  $SiCl_4$  input rate of the OES diagnostic experiment system predicted by thermodynamic equilibrium calculation

The relationship of the intensity ratio  $I_{\text{Si}}/I_{\text{H}}$  and the concentration ratio  $[\text{Si}]/[\text{H}_2]$  can be correlated with  $[\text{Si}]$  and  $[\text{H}_2]$  predicted by equilibrium calculation as given in Fig. 4. The intensity ratio  $I_{\text{Si}}/I_{\text{H}}$  increases linearly with  $[\text{Si}]/[\text{H}_2]$ . This relationship agrees well with Equation (9) thus verifies the equilibrium calculation and the linear correlation between  $I_{\text{Si}}/I_{\text{H}}$  and  $[\text{Si}]/[\text{H}_2]$ .

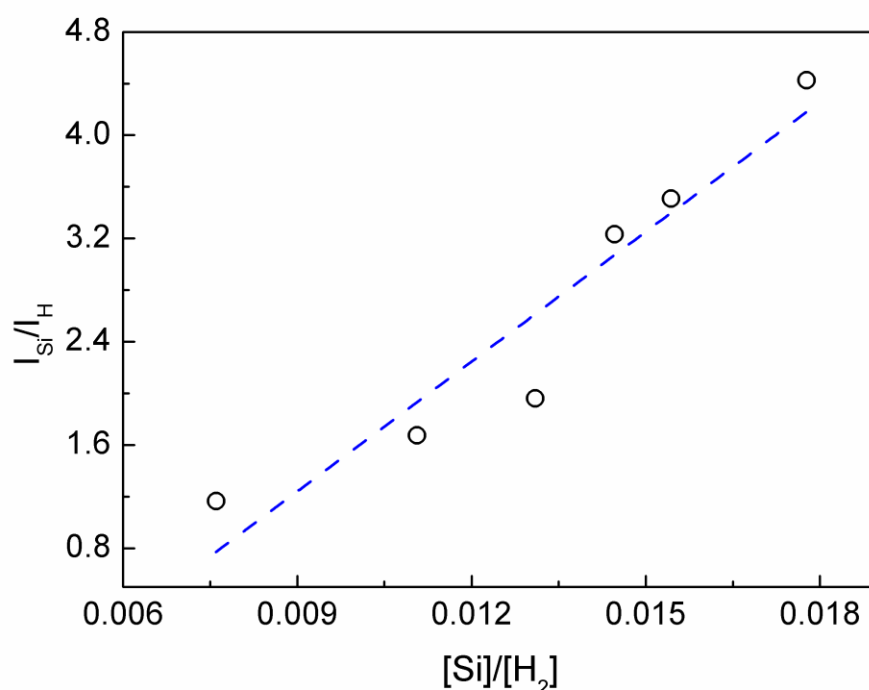


Fig. 4 Verification of the linear correlation between  $I_{\text{Si}}/I_{\text{H}}$  and  $[\text{Si}]/[\text{H}_2]$

## 2. Effect of $\text{SiCl}_4$ input rate on deposition rate and product properties

In our previous work, the high rate deposition of nc-Si:H was successfully realized and product properties have been characterized.<sup>14</sup> In this work, the thermodynamic equilibrium calculation method is used to give a better understanding of the effect of  $\text{SiCl}_4$  input rate on the deposition rate of nc-Si:H and product properties.

The calculated gas phase composition of different  $\text{SiCl}_4$  input rate at operation parameters of

nc-Si:H deposition experiments ( $\text{SiCl}_4$  input rate was changed from 0.05 to 0.13 mol h<sup>-1</sup> and the flow rate of  $\text{H}_2$  was fixed at 2.67 mol h<sup>-1</sup>) is shown in Fig. 5 based on the assumption of thermodynamic equilibrium. Since the equilibrium state of Si-H-Cl system depends only upon the initial and final states of the system, Fig. 5 can be treated as the low  $\text{H}_2/\text{SiCl}_4$  mole ratio part of Fig. 3. Fig. 5 is given here for the detail view of this part. Major silicon related species in the gas phase are SiCl, Si,  $\text{SiCl}_2$ , SiH and SiHCl as can be seen from Fig. 5. The input amount of  $\text{H}_2$  is more than ten times of the input amount of  $\text{SiCl}_4$  at the high  $\text{H}_2$  dilution ratio of the nc-Si:H deposition experiment. So the decrease of  $[\text{H}_2]$  due to reaction consumption is little. Thus, the effect of  $\text{SiCl}_4$  input rate on  $[\text{H}_2]$  is small.

The kinetic process of the chlorosilane and silane decomposition to deposit silicon has been widely studied and showed that the decomposition of the absorbed species from the gas phase finally leads to the deposition of silicon.<sup>29-31</sup> Absorbed atomic chlorine has an etching effect on silicon, which hampers the deposition process. The nc-Si:H fabrication is a competition of deposition and etching. Therefore, the deposition rate of nc-Si:H can be simply estimated using the following expression

$$r_{\text{dep}} = k_{\text{dep}}[\text{silicon related species}] - k_{\text{etch}}[\text{chlorine related species}], \quad (10)$$

where  $k_{\text{dep}}$  and  $k_{\text{etch}}$  are the rate constants for deposition and etching respectively, [silicon related species] is the silicon related species concentration of the gas phase and [chlorine related species] is the chlorine related species concentration of the gas phase.

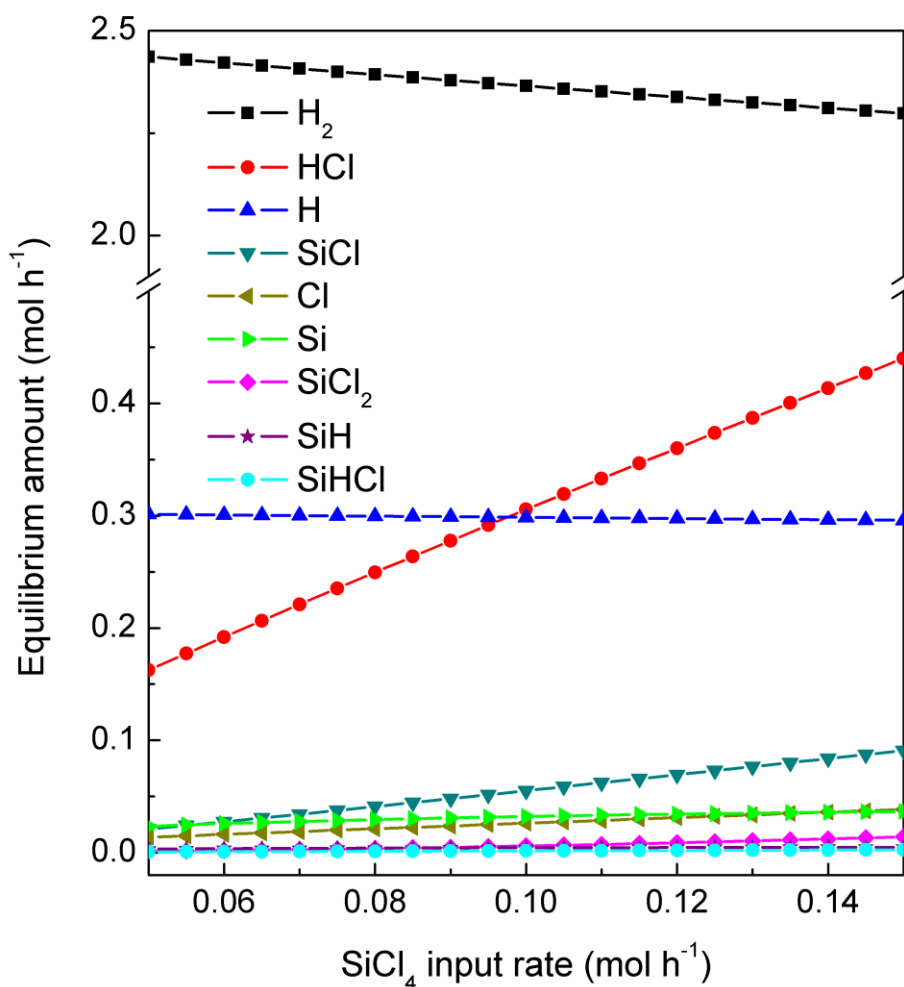


Fig. 5 Gas phase composition at different  $\text{SiCl}_4$  input rate of the nc-Si:H deposition experiment system predicted by thermodynamic equilibrium calculation

The relationship between the amount of silicon related species in the gas phase predicted by equilibrium calculation and the deposition rate is shown in Fig. 6. The deposition rate is almost proportional to the silicon related species amount in the gas phase, which means that the etching effect of the chlorine related species in the nc-Si:H deposition process is negligible according to Equation (10). This can be explained by the role of atomic hydrogen in the reaction system. A

sufficient amount of atomic hydrogen in the gas phase can accelerate the decomposition of silicon related species to deposit silicon<sup>32</sup> and can also enable efficient surface coverage by bonded hydrogen so as to weaken the formation of atomic chlorine and then the etching effect<sup>1</sup>. This shows the advantage of utilizing high H<sub>2</sub> dilution ratio in the nc-Si:H deposition system with SiCl<sub>4</sub> as precursor.

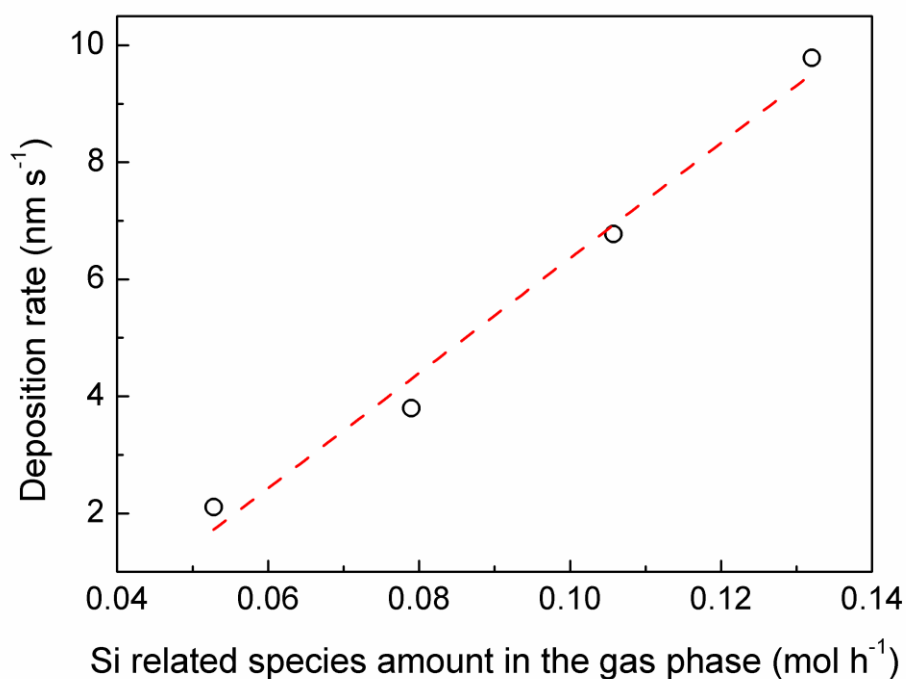


Fig. 6 Relationship between nc-Si:H deposition rate and the silicon related species amount in the gas phase

Furthermore, the effect of SiCl<sub>4</sub> input rate on nc-Si:H product properties is also studied. As can be seen from Fig. 5, the increase of SiCl<sub>4</sub> input rate leads to the change of silicon related species amount in the gas phase, which is found to be the main factor affecting product properties. The relationships between the amount of silicon related species in the gas phase and the grain size

as well as the crystalline fraction of the product are shown in Figs. 7 and 8. Both grain size and crystalline fraction correlate linearly with silicon related species amount. The deposition of silicon leads to the growth of silicon crystalline grain. The growth rate of the crystalline grain is proportional to the silicon deposition rate thus proportional to silicon related species amount in the gas phase. That means larger amount of silicon related species results in higher grain growth rate. Since the average residence time of the grains is nearly the same at different  $\text{SiCl}_4$  input rate, a larger average grain size will be seen at higher silicon related species amount in the gas phase.

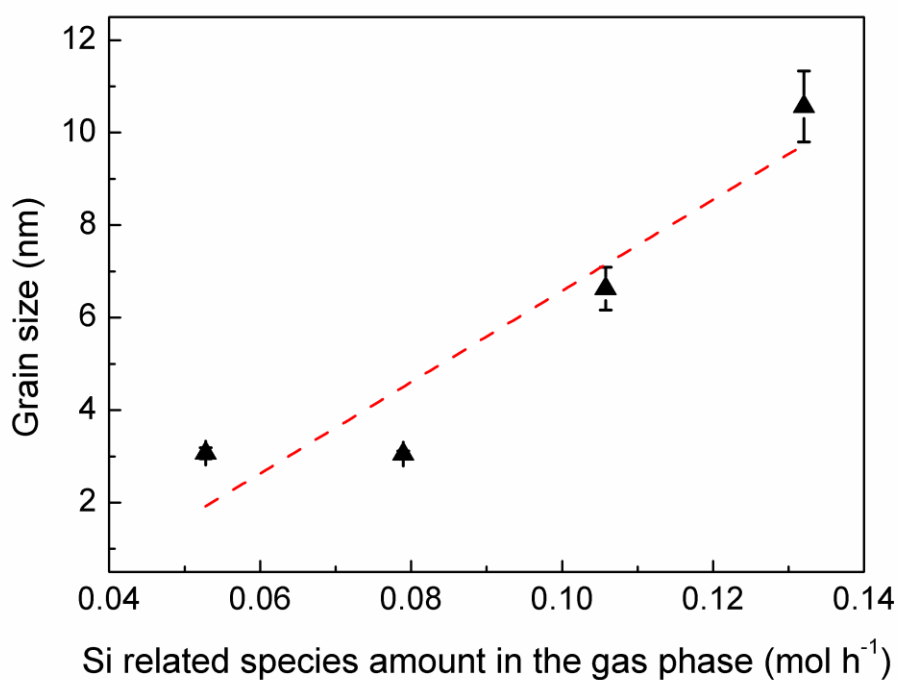


Fig. 7 Relationship between the grain size of nc-Si:H and the silicon related species amount in the gas phase

The relationship between crystalline fraction and the amount of silicon related species in the gas phase is shown in Fig. 8. Surface hydrogen plays an important role in the crystallization

process.<sup>1,33</sup> Local heating produced by recombination reactions of surface hydrogen intensifies the crystallization process,<sup>34,35</sup> while the etching effect of hydrogen on the amorphous phase further improves the crystalline fraction<sup>36</sup>. As discussed before, hydrogen remains at a high concentration for the high H<sub>2</sub> dilution ratio applied in this work. Thus, its etching effect on amorphous phase almost keeps at the same level at different SiCl<sub>4</sub> input rate. As the deposition rate rises with increasing silicon related species amount in the gas phase, more crystalline phase is formed and appears in the nc-Si:H product. This leads to the linear correlation between crystalline fraction and silicon related species amount in the gas phase at a high H<sub>2</sub> dilution ratio. However, the improvement of the crystalline fraction is small. The high and uncontrollable ion energy originating from the stochastic fluctuations of large sheath potentials in the ICP RF plasma may lead to the relatively low crystalline fraction of the nc-Si:H product.<sup>34</sup>

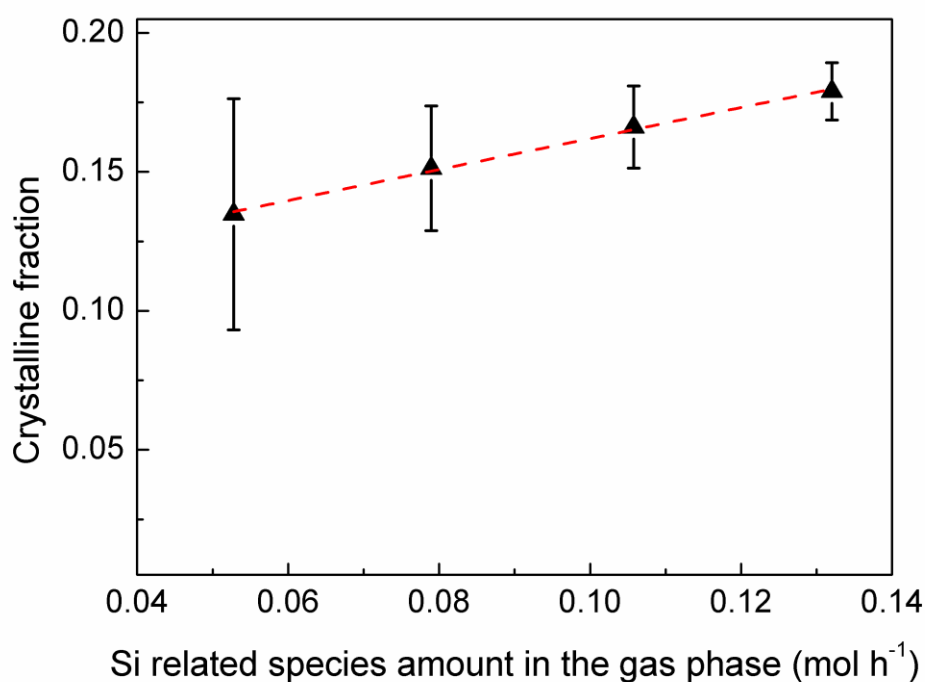


Fig. 8 Relationship between the crystalline fraction of nc-Si:H and the silicon related species

amount in the gas phase

As a summary, the amount of silicon related species in the gas phase is found to be the main factor affecting nc-Si:H deposition rate and product properties. High SiCl<sub>4</sub> input rate leads to large amount of silicon related species in the gas phase, thus benefits the deposition rate and crystalline fraction at the high H<sub>2</sub> dilution ratio of the nc-Si:H deposition experiments. If the SiCl<sub>4</sub> input rate continues increasing, the situation of deposition reactions will change. Gas phase composition at a high SiCl<sub>4</sub> input rate and a low H<sub>2</sub> dilution ratio predicted by equilibrium calculation is given in Fig. 9. The amount of chlorine related species keeps going up while the amount of H<sub>2</sub> and atomic hydrogen keeps going down with more chlorine atom entering the system. The amount of atomic chlorine exceeds the amount of atomic hydrogen when SiCl<sub>4</sub> input rate reaches 0.95 mol h<sup>-1</sup> with a H<sub>2</sub> dilution ratio of 2.81. The surface coverage of atomic hydrogen turns insufficient. And the etching effect of atomic chlorine is no longer negligible with more atomic chlorine absorbed on the surface. Thus, the linear relationship between the deposition rate and the silicon related species concentration in the gas phase becomes false at high SiCl<sub>4</sub> input rate. Both the correlations of grain size and crystalline fraction have to be rebuilt at high SiCl<sub>4</sub> input rate and low H<sub>2</sub> dilution ratio.

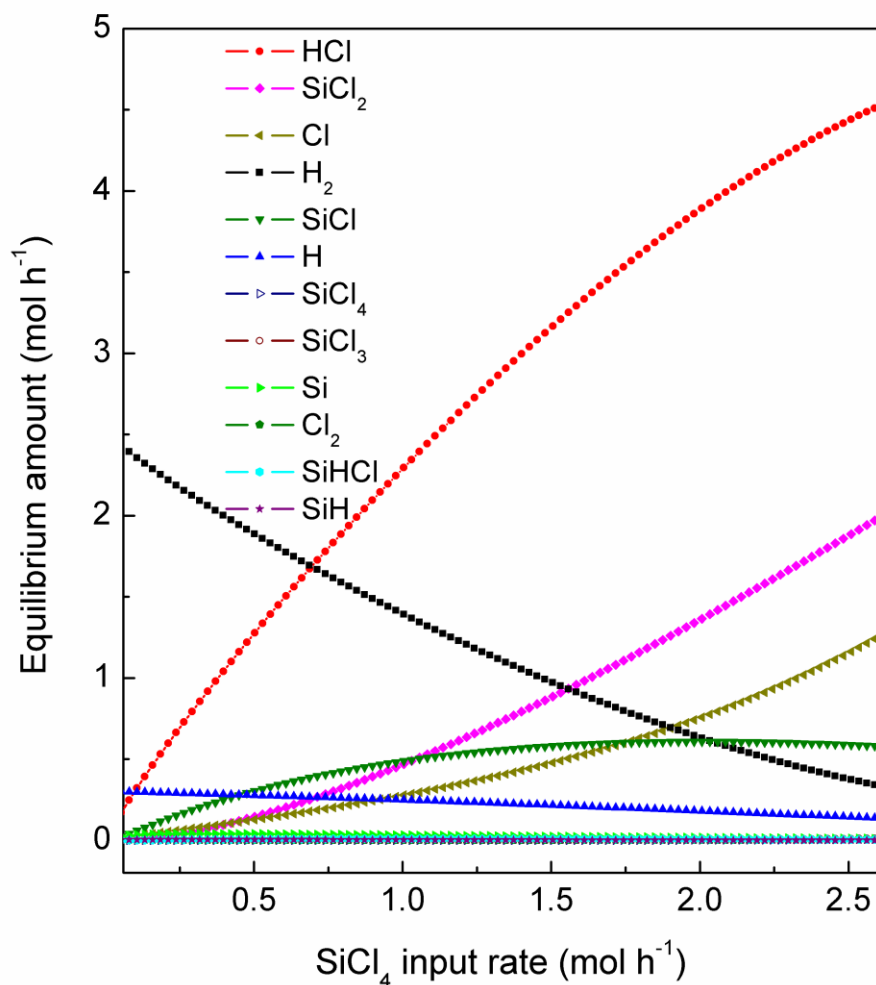


Fig. 9 Gas phase composition at high SiCl<sub>4</sub> input rate predicted by equilibrium calculation

## Experimental

### 1. OES diagnostic

The schematic diagram of the APTPECVD apparatus is shown in Fig. 10. The plasma jet is generated by a RF generator with a frequency of 10~13 MHz and a power up to 10 kW. SiCl<sub>4</sub> diluted by H<sub>2</sub> is used as precursor. Ar is the plasma gas and sheath gas as well. During the OES

diagnostic experiment, the input rate of  $\text{SiCl}_4$  is changed from  $0.05 \text{ mol h}^{-1}$  to  $0.52 \text{ mol h}^{-1}$ , while the input rate of  $\text{H}_2$  is fixed at  $3.65 \text{ mol h}^{-1}$ .  $\text{SiCl}_4$  is a volatile liquid under room temperature. The  $\text{SiCl}_4$  precursor was transferred into a plastic injector in the fuming cupboard and pumped into the reaction system using an injection pump. The OES detector, placed below the RF coils at the same altitude of the plasma plume outside the quartz tube, is connected to the spectrometer via a four-channel optic fiber. The resolution of each channel is given in Table 1. The emission within ultraviolet, visible and near-infrared range is then recorded. Detailed information of the experimental system can be also found in our previous work<sup>14</sup>.

Table 1 The resolution of the four-channel spectrometer

Wavelength range (nm)	Resolution (nm)
200-360	0.12
360-505	0.1
505-625	0.09
625-820	0.15

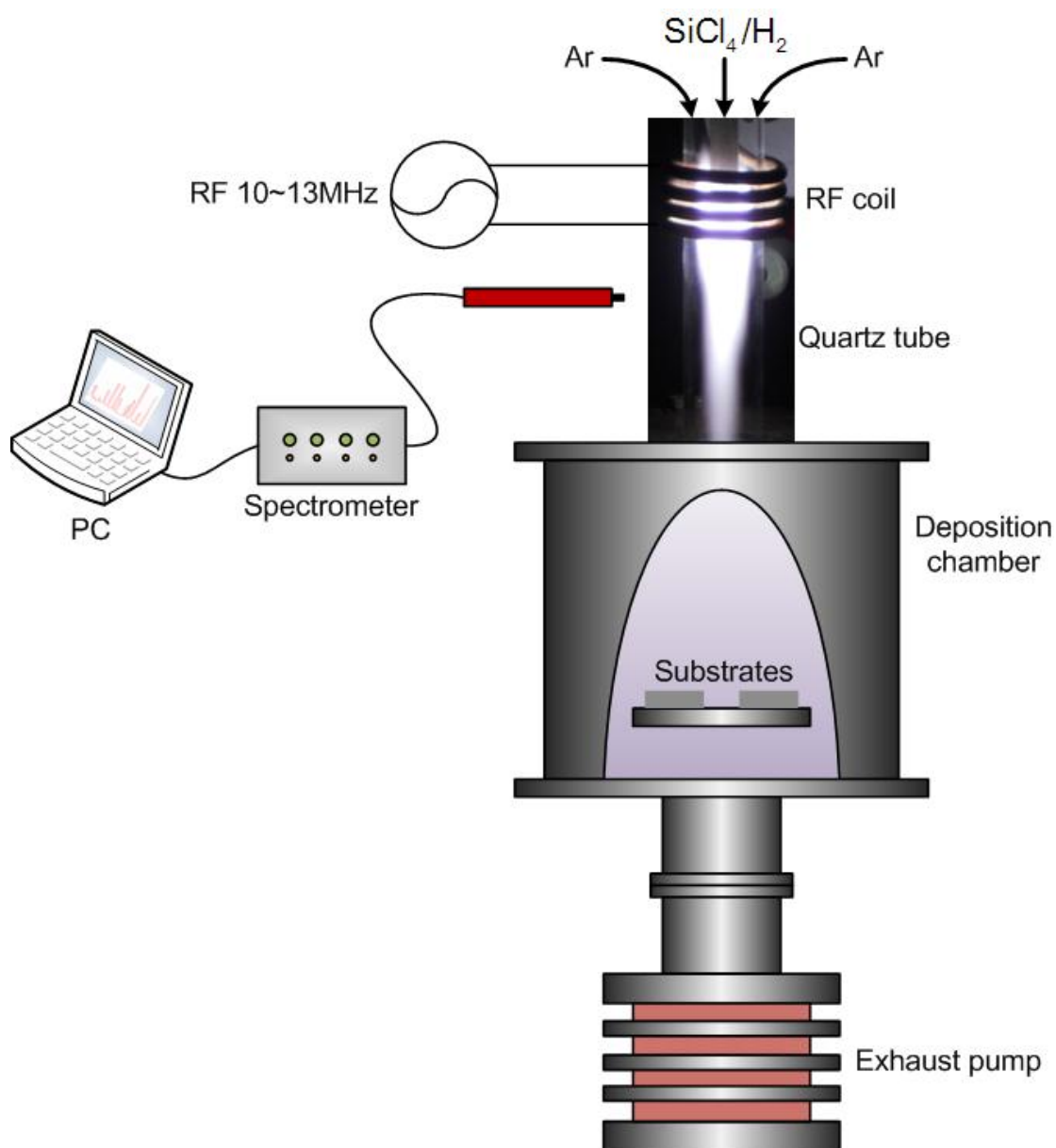


Fig. 10 Sketch of the APTPECVD and OES diagnostic system

## 2. Thermodynamic equilibrium analysis

The thermodynamic analysis of the gas phase equilibrium composition was carried out using the element potential method based on the minimization of Gibbs free energy, which can be referred to the similar work on thermodynamic equilibrium analysis of C-H-O system by Yan et al.<sup>25</sup>. The gas phase species were assumed to include Si, SiCl, SiCl<sub>2</sub>, SiCl<sub>3</sub>, SiCl<sub>4</sub>, SiH, SiH<sub>2</sub>, SiH<sub>3</sub>,

SiH<sub>4</sub>, SiHCl, SiHCl<sub>3</sub>, SiH<sub>2</sub>Cl<sub>2</sub>, SiH<sub>3</sub>Cl, H, H<sub>2</sub>, HCl, Cl and Cl<sub>2</sub>. The equilibrium composition was calculated under an estimated temperature of the OES observation point. Based on the simulation results reported<sup>9, 37</sup> and the results of infrared temperature measurement, the temperature of the OES observation point was set to be 2700 K. This temperature is relatively low compared to the temperature of the plasma zone. It is a volume average of the system temperature at the OES observation point. And the equilibrium composition in the thermodynamic equilibrium calculation is also a macroscopic average value of the gas phase composition. The emission intensity of Si (288.08 nm) signal is proportional to the atomic silicon amount calculated under thermodynamic equilibrium assumption at 2700 K as shown in Fig. 11. Since the SiCl<sub>4</sub> input amount is relatively small compared with the amount of plasma gas, its effect on electron density,  $n_e$ , could be negligible. Therefore, the emission intensity of atomic silicon is approximately linearly correlated with the atomic silicon concentration in gas phase according to Equation (7). The consistency between Fig. 11 and Equation (7) proves the reasonability of the estimation of the gas phase temperature.

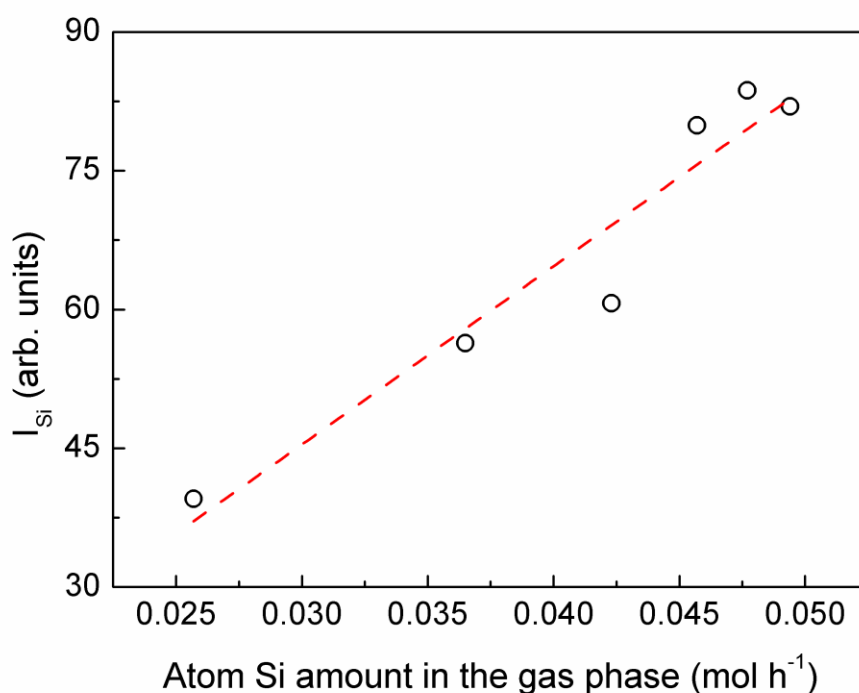


Fig. 11 Relationship between emission intensity of atomic silicon and the atomic silicon amount in the gas phase calculated under thermodynamic equilibrium assumption at 2700 K

## Conclusion

nc-Si:H is a promising alternative for conventional crystalline silicon material in photovoltaic industry. The deposition of nc-Si:H at high rate has been successfully realized and the deposition reactions was studied in this work. The effect of SiCl<sub>4</sub> input rate on the gas phase reaction during the thermal plasma enhanced nc-Si:H deposition process has been analyzed using OES diagnostic and thermodynamic equilibrium calculation. Emission lines of excited species including Si<sup>\*</sup>, H<sup>\*</sup> and Ar<sup>\*</sup> were observed. The correlation of emission intensity and gas phase composition was built under the kinetic mechanism of SiCl<sub>4</sub> decomposition in Ar-H<sub>2</sub> plasma. The thermodynamic equilibrium analysis assisted to better understand the effect of SiCl<sub>4</sub> input rate on nc-Si:H

deposition rate and product properties such as grain size and crystalline fraction. The equilibrium calculation method was verified by OES diagnostic results. The amount of silicon related species in the gas phase was found to be the main factor affecting the deposition rate and product properties and their linear relationship at high H<sub>2</sub> dilution ratio was discovered. Etching effect of chlorine related species was demonstrated negligible under the high H<sub>2</sub> dilution ratio applied in this work. Owing to the severe environment at ultra-high temperatures and integrated multiple processes in milliseconds, direct measurement inside the thermal plasma deposition reactor can hardly be implemented. By combining OES diagnostic and thermodynamic equilibrium calculation, deposition process in the thermal plasma reactor was further analyzed. The correlation between gas phase composition and product properties in this work can help to optimize the deposition parameters and the analyzing method proposed can be applied to characterize other processes in thermal plasma.

## Acknowledgement

This study is supported by the National Basic Research Program of China (973 Program no. 2012CB720301), the National Natural Science Foundation of China (NSFC) under grant no. 21176137.

## Notes and references

\* *Department of Chemical Engineering, Tsinghua University, Beijing, China.*

*Fax: 86-10-62772051; Tel: 86-10-62794468; E-mail: yicheng@tsinghua.edu.cn*

1. Q. Cheng, S. Xu and K. K. Ostrikov, *J. Mater. Chem.*, 2009, **19**, 5134-5140.

2. J. Meier, R. Fluckiger, H. Keppner and A. Shah, *Appl. Phys. Lett.*, 1994, **65**, 860-862.
3. C. H. Lee, A. Sazonov and A. Nathan, *Appl. Phys. Lett.*, 2005, **86**, 222106.
4. C. H. Lee, A. Sazonov, A. Nathan and J. Robertson, *Appl. Phys. Lett.*, 2006, **89**, 252101.
5. A. Shah, J. Meier, E. Vallat-Sauvain, N. Wyrsh, U. Kroll, C. Droz and U. Graf, *Sol. Energ. Mat. Sol. C.*, 2003, **78**, 469-491.
6. V. L. Dalal, J. Graves and J. Leib, *Appl. Phys. Lett.*, 2004, **85**, 1413-1414.
7. K. K. Ostrikov, U. Cvelbar and A. B. Murphy, *J. Phys. D Appl. Phys.*, 2011, **44**, 174001.
8. K. K. Ostrikov and A. B. Murphy, *J. Phys. D Appl. Phys.*, 2007, **40**, 2223-2241.
9. S. L. Girshick, C. P. Chiu, R. Muno, C. Y. Wu, L. Yang, S. K. Singh and P. H. McMurry, *J. Aerosol. Sci.*, 1993, **24**, 367-382.
10. M. Shigeta and A. B. Murphy, *J. Phys. D Appl. Phys.*, 2011, **44**, 174025.
11. M. Keidar, A. Shashurin, J. A. Li, O. Volotskova, M. Kundrapu and T. S. Zhuang, *J. Phys. D Appl. Phys.*, 2011, **44**, 174006.
12. I. Levchenko, O. Volotskova, A. Shashurin, Y. Raitses, K. K. Ostrikov and M. Keidar, *Carbon*, 2010, **48**, 4570-4574.
13. K. K. Ostrikov, E.C. Neyts and M. Meyyappan, *Adv. Phys.*, 2013, **62**, 113-224.
14. T. F. Cao, H. B. Zhang, B. H. Yan and Y. Cheng, *RSC Adv.*, 2013, **3**, 20157-20162.
15. L. Zhang, J. Gao, J. Xiao, L. Wen, J. Gong and C. Sun, *Phys. Status. Solidi. A*, 2012, **209**, 1080-1084.
16. F. J. Kampas, *J. Appl. Phys.*, 1983, **54**, 2276-2280.
17. G. Cicala, M. Losurdo, P. Capezzuto and G. Bruno, *Plasma Sources Sci. T.*, 1992, **1**, 156-165.
18. F. Bourg, S. Pellerin, D. Morvan, J. Amouroux and J. Chapelle, *Sol. Energ. Mat. Sol. C.*, 2002, **72**, 361-371.
19. L. Feitknecht, J. Meier, P. Torres, J. Zurcher and A. Shah, *Sol. Energ. Mat. Sol. C.*, 2002, **74**, 539-545.
20. S. Yokoyama, M. Hirose and Y. Osaka, *Jpn. J. Appl. Phys.*, 1981, **20**, L117-L120.
21. Y. Fukuda, Y. Sakuma, C. Fukai, Y. Fujimura, K. Azuma and H. Shirai, *Thin Solid Films*, 2001, **386**, 256-260.
22. L. P. Hunt and E. Sirtl, *J. Electrochem. Soc.*, 1972, **119**, 1741.
23. E. Sirtl, L. P. Hunt and D. H. Sawyer, *J. Electrochem. Soc.*, 1974, **121**, 919-925.
24. S. M. Eichfeld, H. T. Shen, C. M. Eichfeld, S. E. Mohny, E. C. Dickey and J. M. Redwing, *J. Mater. Res.*, 2011, **26**, 2207-2214.
25. B. H. Yan, P. C. Xu, Y. Jin and Y. Cheng, *Chem. Eng. Sci.*, 2012, **84**, 31-39.
26. H. H. Richter, A. Wolff, B. Tillack and T. Skaloud, *Mat. Sci. Eng. B-Solid*, 1994, **27**, 39-45.
27. T. Sakurai, S. Kobayashi, J. Ogura, Y. Inoue and H. Hori, *Aust. J. Phys.*, 1995, **48**, 515-526.
28. X. S. Li, N. Wang, J. H. Yang, Y. Wang and A. M. Zhu, *Plasma Sci. Technol.*, 2011, **13**, 567-570.
29. S. P. Walch and C. E. Dateo, *J. Phys. Chem. A*, 2001, **105**, 2015-2022.
30. G. Valente, C. Cavallotti, M. Masi and S. Carra, *J. Cryst. Growth*, 2001, **230**, 247-257.
31. S. Ravasio, M. Masi and C. Cavallotti, *J. Phys. Chem. A*, 2013, **117**, 5221-5231.
32. M. Sumiya, T. Akizuki, K. Itaka, M. Kubota, K. Tsubouchi, T. Ishigaki and H. Koinuma, Proceedings of the 11th Asia Pacific Conference on Plasma Science and Technology and 25th Symposium On Plasma Science for Materials, Bristol, 2013.
33. A. M. Funde, N. A. Bakr, D. K. Kamble, R. R. Hawaldar, D. P. Amalnerkar and S. R. Jadkar, *Sol. Energ. Mat. Sol. C.*, 2008, **92**, 1217-1223.

34. M. Kondo, S. Suzuki, Y. Nasuno, M. Tanda and A. Matsuda, *Plasma Sources Sci. T.*, 2003, **12**, S111-S116.
35. K. K. Ostrikov, *Rev. Mod. Phys.*, 2005, **77**, 489-511.
36. Y. L. He, C. Z. Yin, G. X. Cheng, L. C. Wang, X. N. Liu and G. Y. Hu, *J. Appl. Phys.*, 1994, **75**, 797-803.
37. M. Desilets, J. F. Bilodeau and P. Proulx, *J. Phys. D Appl. Phys.*, 1997, **30**, 1951-1960.